Quaternary International 399 (2016) 190–197

Contents lists available at ScienceDirect

Quaternary International

journal homepage: www.elsevier.com/locate/quaint

Leaf wax *n*-alkane distributions in Chinese loess since the Last Glacial Maximum and implications for paleoclimate

Yangyang Li [a, b], Shiling Yang [a, *], Xu Wang [a], Jianfang Hu [c], Linlin Cui [a], Xiaofang Huang [a, b], Wenying Jiang [a]

[a] Key Laboratory of Cenozoic Geology and Environment, Institute of Geology and Geophysics, Chinese Academy of Sciences, Beijing 100029, China
[b] University of Chinese Academy of Sciences, Beijing 100049, China
[c] State Key Laboratory of Organic Geochemistry, Guangzhou Institute of Geochemistry, Chinese Academy of Sciences, Guangzhou 510640, China

ARTICLE INFO

Article history:
Available online 14 May 2015

Keywords:
n-Alkane
Chinese loess
Holocene
Last Glacial Maximum
Paleoclimate

ABSTRACT

Leaf wax *n*-alkanes have been recently introduced into loess deposits for paleovegetation and paleoclimate reconstruction. However, the paleoclimate significance of some *n*-alkane parameters such as chain-length ratios (L/H, C_{27}/C_{31}, C_{29}/C_{31}, and $(C_{27}+C_{29})/(C_{31}+C_{33})$) remains to be clarified. In order to evaluate the validity of those proxies in loess deposits, leaf wax *n*-alkanes were analyzed from a northwest-southeast transect on the Chinese Loess Plateau since the Last Glacial Maximum (LGM). The *n*-alkanes show a bimodal distribution between C_{14} and C_{33} with Carbon number maxima (C_{max}) at C_{14} or C_{16}, and at C_{31} or C_{33}, indicative of both terrestrial plant and microbial origin. L/H variations are in good agreement with climate changes both temporally and spatially, i.e. the higher L/H ratio the warmer and wetter climate and vice versa. Therefore, the L/H ratio in Chinese loess can serve as an efficient proxy for paleoclimate. By comparing long-chain *n*-alkane ratios with pollen records, we suggest that the generally used woody plant proxies (C_{27} and C_{29}) and grass proxies (C_{31} and C_{33}) are not applicable to Chinese loess. As the Chinese Loess Plateau was dominated by herbs in both the LGM and the Holocene, the long-chain *n*-alkane ratios may mainly reflect changes in the species composition of local vegetation. For a better understanding of leaf wax *n*-alkanes in Chinese loess, further studies are required to investigate the *n*-alkane distributions in both the major plant species and their associated surface soils on the Chinese Loess Plateau.

1. Introduction

Leaf wax forms a hydrophobic layer covering aerial plant organs, which serves as a waterproof barrier protecting plants against desiccation, ultraviolet radiation, and pathogens (Eglinton and Hamilton, 1967; Kolattukudy, 1976a). The waxy coats typically are complex mixtures of mainly *n*-alkanes, *n*-alcohols, *n*-alkanoic acids, and wax esters (Eglinton and Hamilton, 1967; Kolattukudy, 1976a; Eglinton and Eglinton, 2008). Among these, *n*-alkanes have attracted particular interest for paleoenvironmental research, as they can be easily identified and isolated from a variety of geologic materials and are relatively robust to geologic alteration.

In the past decade, some *n*-alkane parameters such as chain-length ratios have been introduced into loess deposits for paleovegetation and paleoclimate studies (Xie et al., 2003, 2004; Zhang et al., 2003, 2006; Liu and Huang, 2005, 2008; Bai et al., 2009; Zech et al., 2009a, b, 2010; 2012; Buggle et al., 2010; Gocke et al., 2010). Some researchers suggested that C_{31} and C_{33} represent input from grasses while C_{27} and C_{29} represent input from woody plants (trees and shrubs) (Cranwell, 1973; Meyers and Ishiwatari, 1993; Schwark et al., 2002; Meyers, 2003; Bai et al., 2009). For this reason, ratios constructed from long-chain *n*-alkanes (e.g., C_{27}/C_{31}, C_{29}/C_{31}, and $(C_{27}+C_{29})/(C_{31}+C_{33})$) have been increasingly used in loess deposits to estimate the relative contribution of woody plants and grasses (Yang et al., 2006; Zhong et al., 2007; Zhang et al., 2008; Zeng et al., 2011). However, the validity of these *n*-alkane ratios has been challenged by investigations of *n*-alkanes in woody plants, grasses, and their associated soils from China and North America, which indicate that they all have highly variable but significant amounts of C_{29} and C_{31} (Rao et al., 2011; Luo et al., 2012; Bush and McInerney, 2013). In addition, the

* Corresponding author.
E-mail address: yangsl@mail.iggcas.ac.cn (S. Yang).

http://dx.doi.org/10.1016/j.quaint.2015.04.029
1040-6182/

paleoclimate significance of L/H ratio (the ratio of low- to high-molecular-weight *n*-alkanes) remains to be clarified (Xie et al., 2004; Zeng et al., 2011). Therefore, the paleoenvironmental implications of *n*-alkanes in loess deposits need to be carefully evaluated.

On the Chinese Loess Plateau, a pronounced spatial climatic gradient similar to the present pattern existed in both glacials and interglacials (Derbyshire et al., 1995; Yang and Ding, 2003, 2008; Yang et al., 2012, 2014; Jiang et al., 2013, 2014). This provides a unique opportunity to evaluate the paleoenvironmental implications of *n*-alkanes in loess deposits through temporal and spatial comparisons. Here we present leaf wax *n*-alkane records from a northwest–southeast loess transect in the Chinese Loess Plateau since the Last Glacial Maximum (LGM), with the aim of exploring the paleoenvironmental implications of chain-length ratios in Chinese loess.

2. Setting and stratigraphy

Our study transect runs northwest–southeast from Huanxian near the Mu Us desert margin, to Lingbao in the southeast Loess Plateau. Three loess sections located at Huanxian (36.39°N, 107.14°E), Fuxian (36.01°N, 109.18°E), and Lingbao (34.34°N, 110.50°E) were sampled (Fig. 1). The modern climate of the study area is characterized by seasonal alternations of wet, warm summer monsoon and dry, cold winter monsoon. From Huanxian to Lingbao, there is a positive southeastward gradient in both mean annual temperature (from ~8 to ~13 °C) and mean annual precipitation (from ~380 to ~630 mm), with ~60–80% of the precipitation concentrated in summer season.

All the sections consist of the Holocene soil S0 and the upper part of loess unit L1. The Holocene soil S0 is dark in colour because of its relatively high organic matter content. S0 can be approximately classified as a Calcic Chernozem at Huanxian, a Luvic Phaeozem at Lingbao, and an intergrade between them at Fuxian (FAO, 1988), and displays a southeasterly increase in pedogenic development, which coincides with the modern spatial climatic gradient.

Radiocarbon (Liu et al., 1994) and OSL (Huang et al., 2006; Lu et al., 2007) dating have provided an age of ~11–9 ka for the base of S0 soil unit and an age of ~3 ka for the top of S0. The loess unit L1 is yellowish in colour and massive in structure, deposited during the last glacial period. The loess unit L1 can be divided into five subunits, termed L1-1, L1-2, L1-3, L1-4, and L1-5. L1-2 and L1-4 are weakly developed soils, and the other subunits are typical loess horizons. Previous studies have shown that L1-1 is correlated with marine isotope stage (MIS) 2 (~27–11 ka), and L1-2 with the late MIS 3 (~38–27 ka) (Kukla, 1987; Ding et al., 2002; Lu et al., 2007; Yang and Ding, 2014). The stratigraphy of all the sections is correlative in the field, suggesting near-continuous dust accumulation since the last glacial period. To ensure that we used a complete cold–warm cycle for *n*-alkane studies, all the sections were sampled down to loess unit L1-2.

3. Materials and methods

For all the sections, a total of 282 samples were collected at 5–10 cm intervals. Bulk magnetic susceptibility and grain size were measured for all samples using a Bartington MS2 susceptibility meter and a SALD–3001 laser diffraction particle analyzer. About 10 g of each sample was measured for magnetic susceptibility. Ultrasonic pretreatment with addition of a 20% solution of $(NaPO_3)_6$ was used to disperse the samples prior to particle size determination (for details see Ding et al. (1999)).

A total of 30 samples were selected for *n*-alkane analysis. In order to avoid potential contamination during the *n*-alkane extraction, all glassware was sequentially washed with detergent, chromic acid (soaked for 24 h), tap water, and distilled water, and finally annealed at 450 °C for 5 h. Filter papers were Soxhlet extracted with a mixed solvent of dichloromethane and methanol (3:1, v:v) for 72 h prior to use. All samples were dried at 40 °C and ground. An aliquot (80–100 g) of each sample was Soxhlet–extracted with dichloromethane:methanol (3:1, v:v) for 48 h. Total lipid extracts were separated by column silica gel chromatography, and the hydrocarbon fraction was eluted with hexane.

n-Alkanes were identified and quantified using a Konik HRGC 4000B Gas chromatography with flame ionization detector (FID) and a non-polar capillary column (HP-5MS 60 m × 0.25 mm × 0.25 μm) at the Institute of Geology and Geophysics, Chinese Academy of Sciences. The GC oven temperature program initiated

Fig. 1. Map showing the study sites (dots) in the Chinese Loess Plateau.

at 80 °C (held for 2 min), increased at 10 °C/min to 150 °C, and then at 4 °C/min to 290 °C (held for 20 min). Compounds were identified through comparison of retention times with *n*-alkane references (C_7–C_{40}). Compound concentrations were determined by comparing the peak areas of samples with those of the references (C_7–C_{40}) at a concentration of 100 ng/μl.

4. Results

4.1. Magnetic susceptibility and grain size

The alternation of loess and soils is clearly expressed in the grain-size and magnetic susceptibility records (Fig. 2). In the three sections, soil unit S0 is characterized consistently by finer particle size and higher susceptibility values compared with loess unit L1-1 (Fig. 2). In the Huanxian section, the median grain size and the susceptibility values fall in the range 30–48 μm and 30–60 × 10^{-8} m^3/kg for loess unit L1-1, and in the range 20–32 μm and 40–110 × 10^{-8} m^3/kg for the Holocene soil S0. The values are 17–25 μm and 45–100 × 10^{-8} m^3/kg for L1-1 and 9–23 μm and 90–160 × 10^{-8} m^3/kg for S0 at Fuxian, and 18–30 μm and 50–90 × 10^{-8} m^3/kg for L1-1 and 14–28 μm and 60–180 × 10^{-8} m^3/kg for S0 at Lingbao. From Huanxian southeastward to Lingbao along the transect, the median grain size generally decreases and the magnetic susceptibility increases for both loess and soil units. These spatial characteristics coincide with the pattern of a southerly increase in pedogenic development for both loess and soil units (Derbyshire et al., 1995; Yang and Ding, 2003), and with the pattern of the present spatial climatic gradient.

4.2. n-Alkane distributions

n-Alkanes from the three sections range from C_{14} to C_{33} and show a bimodal distribution (Fig. 3). Compounds in the range of C_{14} to C_{19} exhibit no odd- or even-carbon preference with a carbon number maximum (C_{max}) at C_{14} or C_{16}, while those ranging from C_{27} to C_{33} show a strong odd-carbon number predominance with a C_{max} at C_{31} or C_{33} (Fig. 3).

4.3. Temporal and spatial records of n-alkane chain-length ratios

4.3.1. L/H ratios

L/H ratio has been used to indicate the relative input of microorganisms and terrestrial higher plants in soils (Xie et al., 2004; Bai et al., 2006; Wang et al., 2007; Zeng et al., 2011), which was calculated as follows:

$$L/H = \frac{C_{14}+C_{15}+C_{16}+C_{17}+C_{18}+C_{19}}{C_{27}+C_{28}+C_{29}+C_{30}+C_{31}+C_{32}+C_{33}} \quad (1)$$

where C_x is the concentration of the *n*-alkane (C) with x carbons.

From the LGM to the Holocene, L/H ratios increased on average from 0.5 to 0.9 at Huanxian, from 0.3 to 0.8 at Fuxian, and from 0.8 to 3.8 at Lingbao (Fig. 4). From northwest to southeast along the transect, L/H ratios displayed an overall increase in both loess and soil horizons (Fig. 4), consistent with the previous finding that L/H values are generally higher in soils of warm and wet climate than in those of cold and dry conditions (Bai et al., 2006; Wang et al., 2007). The averaged L/H value increases more rapidly southeastwards in the Holocene soil unit (S0) compared to the LGM loess unit (L1-1), with an increase of 2.9 and 0.3, respectively.

4.3.2. Long-chain n-alkane ratios

Long-chain *n*-alkane ratios were calculated as follows:

$$(C_{27}+C_{29})/(C_{31}+C_{33}) = \frac{C_{27}+C_{29}}{C_{31}+C_{33}} \quad (2)$$

$$C_{27}/C_{31} = \frac{C_{27}}{C_{31}} \quad (3)$$

$$C_{29}/C_{31} = \frac{C_{29}}{C_{31}} \quad (4)$$

where C_x is the concentration of the *n*-alkane with x carbons.

Fig. 5 illustrates the temporal and spatial changes in the long-chain *n*-alkane ratios. In the Huanxian and Lingbao sections, all

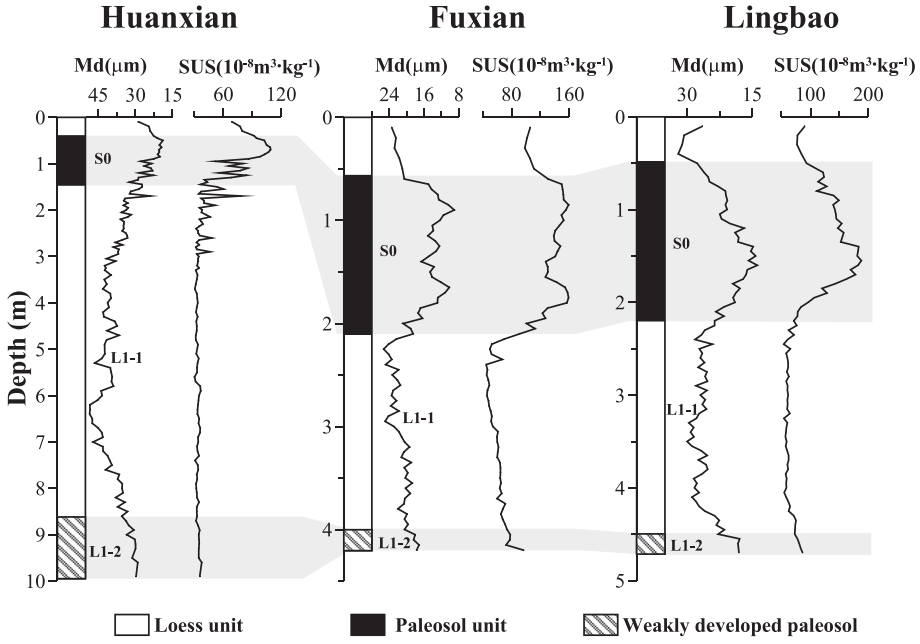

Fig. 2. Stratigraphic column, median grain size (Md), and magnetic susceptibility (SUS) for the Huanxian, Fuxian, and Lingbao sections. The shaded zones indicate the Holocene Optimum (S0) and the late MIS 3 (L1-2).

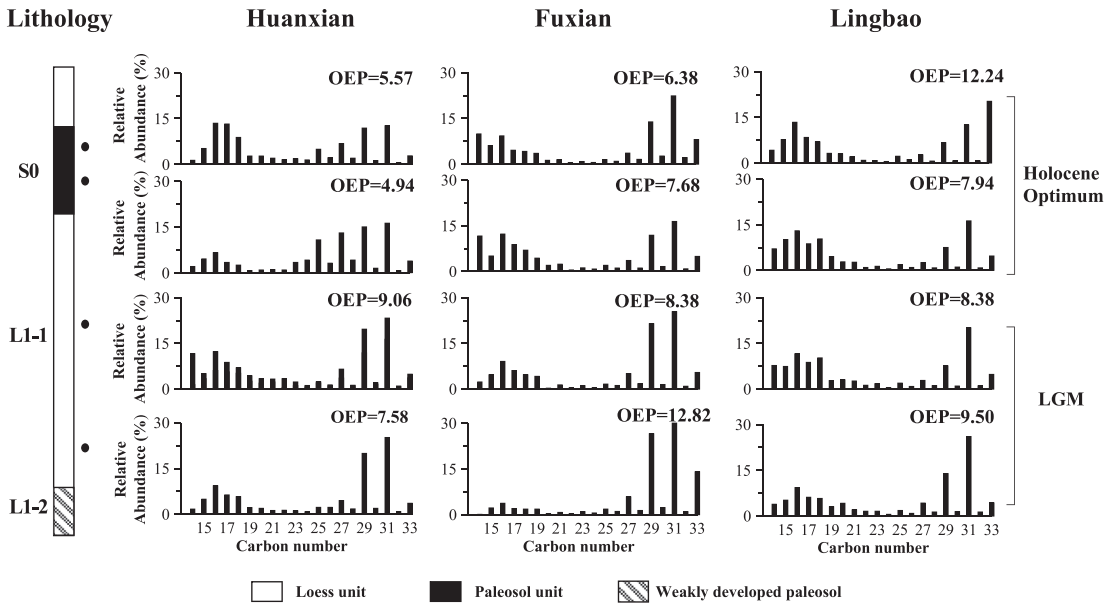

Fig. 3. *n*-Alkane distributions of some representative samples from loess unit L1-1 and soil unit S0 of the loess transect. The associated odd-over-even predominance (OEP) was calculated using the equation of Zech et al. (2009a). $OEP=(C_{27}+C_{29}+C_{31}+C_{33})/(C_{26}+C_{28}+C_{30}+C_{32})$ (5), where C_x is the concentration of the *n*-alkane (C) with x carbons.

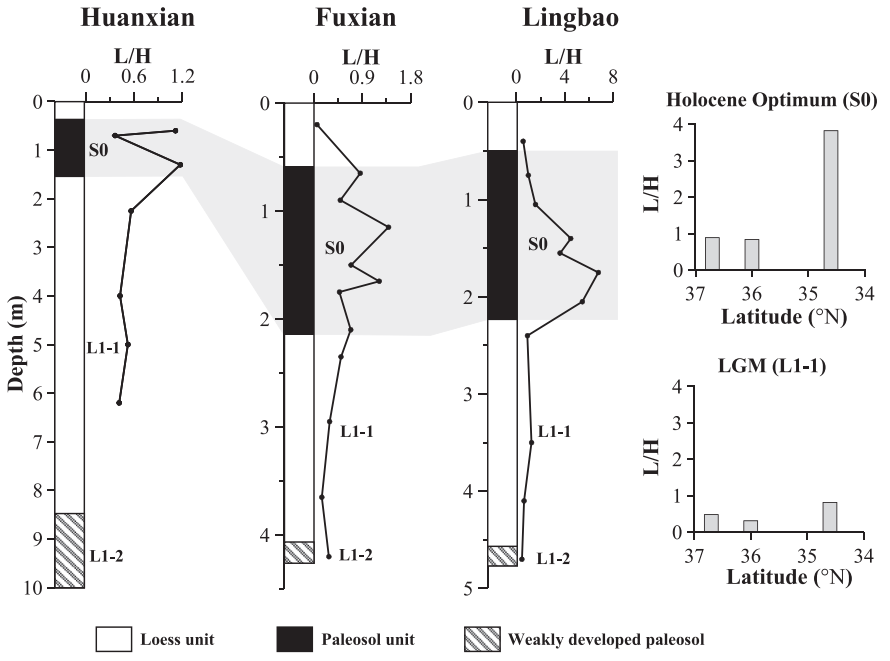

Fig. 4. Temporal and spatial changes in L/H ratios at Huanxian, Fuxian, and Lingbao. The shaded zone indicates the Holocene Optimum.

the *n*-alkane ratios increased significantly from the LGM to the Holocene, while they decreased dramatically in the Fuxian section. Along the loess transect, all the *n*-alkane ratios generally show a southeastward decrease for both loess and soil units. The OEP values in all of the sections exhibited an overall decrease from the LGM to the Holocene (Fig. 5A).

5. Discussion

5.1. Sources of n-alkanes

n-Alkanes in the range of C_{14} to C_{20} without an odd or even carbon number preference are generally indicative of a bacterial and algal input (Han and Calvin, 1969; Albro, 1976; Weete, 1976; Wakeham, 1990). Although abundant algal spores were found in some loess sections, particularly in the southern Loess Plateau (Jiang and Ding, 2005; Jiang et al., 2014), algae typically produce short-chain *n*-alkanes (C_{max} of C_{15}, C_{17}, or C_{19}) (Han and Calvin, 1969; Gelpi et al., 1970; Weete, 1976) different from the cases in our samples (C_{max} of C_{14} or C_{16}; Fig. 3). Therefore the short-chain *n*-alkanes in the three loess sections may be derived mainly from microorganisms.

n-Alkanes typically ranging from C_{25} to C_{35} with a strong odd-over-even carbon chain preference are derived from terrestrial higher plant leaf waxes (Eglinton and Hamilton, 1967; Kolattukudy, 1976b). Long-chain *n*-alkanes with such characteristics were also

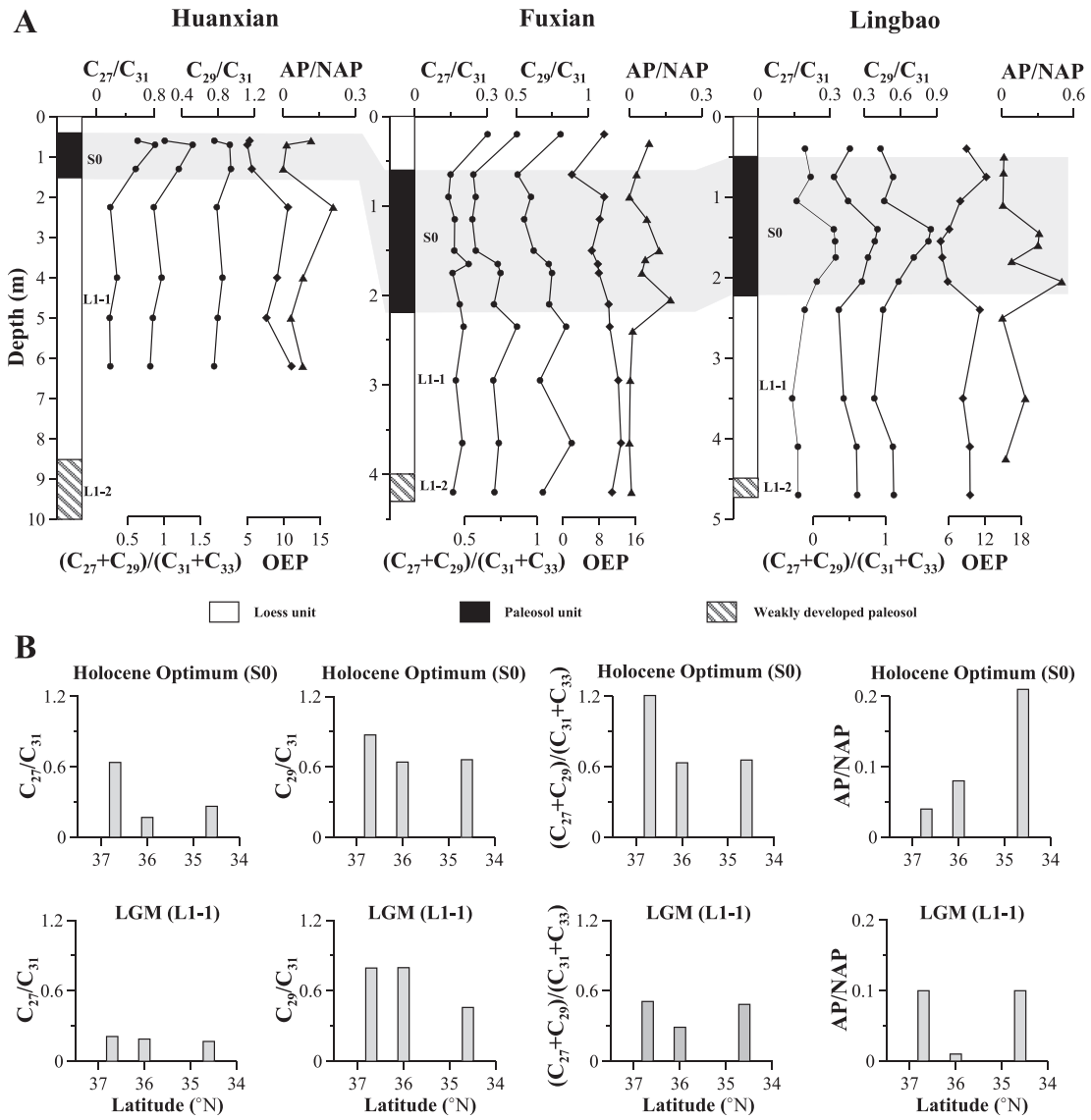

Fig. 5. Comparison of *n*-alkane and pollen records from Huanxian, Fuxian, and Lingbao. A) Changes in long-chain *n*-alkane ratios, OEP, and arboreal pollen/non-arboreal pollen (AP/NAP) values since the LGM. The pollen data are from Jiang et al. (2013, 2014) and Zhao and Ding (2014). The shaded zone indicates the Holocene Optimum. B) Spatial changes in average values of long-chain *n*-alkane ratios and AP/NAP for the LGM and Holocene Optimum.

observed in our samples (Fig. 3), indicating a terrestrial higher plant origin.

Leaf wax *n*-alkanes in the three sections are derived from both microorganisms and higher-plants. Although leaf wax can be transported by wind over a long distance (Gagosian et al., 1981; Conte and Weber, 2002), the eolian leaf wax input into Chinese loess should be very limited as the loess deposits were transported from the arid, barren regions of northwestern China (e.g., Sun, 2002; Yang and Ding, 2008). Therefore, we suggest that the long-chain *n*-alkanes reflect mainly local vegetation.

5.2. L/H ratio as a potential paleoclimate indicator

L/H ratio of soil organic matter can be affected by microbial activities, including the biodegradation of leaf wax *n*-alkanes and the contribution of microbe-derived *n*-alkanes (Johnson and Calder, 1973; Grimalt et al., 1988; Huang et al., 1996; Xie et al., 2003; Bai et al., 2006; Wang et al., 2007). Microbes are generally characterized by short-chain *n*-alkanes (Han and Calvin, 1969; Albro, 1976; Wakeham, 1990; Ladygina et al., 2006), which may partly contribute to short-chain *n*-alkanes in soils (Huang et al., 1996; Freeman and Colarusso, 2001; Xie et al., 2003, 2004). On the other hand, microbes are capable of utilizing long-chain *n*-alkane substrate as a carbon and energy source for metabolism (Rehm and Reiff, 1981; Wentzel et al., 2007), leading to a reduction in long-chain *n*-alkanes. It is therefore inferred that enhanced microbial activities can result in a decrease of L/H ratio. Although some studies (Zaady and Offer, 2010; Svirčev et al., 2013) suggested that a few microorganisms (e.g., *Nostoc* and *Phormidium*) tend to flourish in arid environments, modern soil surveys (Voroney, 2007 and references therein) have shown much greater microbial populations and activities in warm-humid conditions than in cold-dry conditions. This explains the observation that more microbes exist in the paleosols than in the loess layers (Maher and Thompson, 1995; Jia et al., 1996, 2013; Peng et al., 2000).

From the LGM to the Holocene, a significant increase in L/H values is seen in all of the sections (Fig. 4), in accordance with a warmer and wetter climate in the Holocene than in the LGM (Rutter

and Ding, 1993; Liu and Ding, 1998; Yang and Ding, 2008; Jiang et al., 2010). From northwest to southeast along the transect, the L/H value exhibited an overall southeastward increase in both the LGM and the Holocene (Fig. 4), coinciding with the present spatial climatic gradient, namely a southeastward increase in temperature and rainfall. In addition, the spatial gradient of L/H ratio is much steeper in the Holocene than in the LGM (Fig. 4). This is consistent with the conclusion made from colour reflectance (Yang and Ding, 2003), stable isotope (Liu et al., 2005) and pollen records (Jiang et al., 2014), that a steeper climatic gradient occurred in interglacials than in glacials. In this context, the L/H ratio can serve as an efficient proxy for paleoclimate, with high values indicating warm and wet conditions, and vice versa.

5.3. Validity of long-chain n-alkane ratios as proxies for paleovegetation

In order to examine the applicability of previously posited generalities that high long-chain *n*-alkane ratios (C_{27}/C_{31}, C_{29}/C_{31}, and $(C_{27}+C_{29})/(C_{31}+C_{33})$) reflect a relatively high input of woody plants (Cranwell, 1973; Meyers and Ishiwatari, 1993; Schwark et al., 2002; Zhang et al., 2006; Bai et al., 2009), a comparison was made between the *n*-alkane and pollen records for the three sections (Fig. 5). In the Huanxian section, the long-chain *n*-alkane ratios were higher in the Holocene than in the LGM, whereas higher OEP and arboreal pollen/non-arboreal pollen (AP/NAP) values were seen in the LGM than in the Holocene. In contrast, the Holocene soil S0 in the Fuxian section shows lower long-chain *n*-alkane ratios and OEP values but higher AP/NAP values than the glacial loess unit L1-1. In the Lingbao section, the long-chain *n*-alkane ratios were higher in the Holocene than in the LGM, showing a similar pattern to AP/NAP but an opposite pattern to OEP. For a spatial view of the Loess Plateau, all of the long-chain *n*-alkane ratios exhibited an overall decrease from northwest to southeast during the LGM, whereas the AP/NAP ratio did not show any regular spatial pattern (Fig. 5). During the Holocene, the three *n*-alkane ratios decreased southeastwards, whereas the AP/NAP ratio displayed an opposite spatial pattern. It is thus evident that the long-chain *n*-alkane ratio variations cannot be explained by the AP/NAP changes.

Microbial degradation tends to lower the OEP values (Zech et al., 2009a, 2010, 2012; Buggle et al., 2010). Our results exhibited lower OEP values in the Holocene than in the LGM (Fig. 5A), indicating that warm-wet interglacial conditions greatly favor degradation of soil organic matter. However, the observed long-chain *n*-alkane ratio changes (Fig. 5A) cannot be explained by the organic matter degradation. This is because we found no consistent relationship between OEP and long-chain *n*-alkane ratio records for the three sections despite that all the sites were dominated by steppe vegetation throughout the study interval (Jiang et al., 2014; Zhao and Ding, 2014).

Previous studies demonstrate that Chinese Loess Plateau was dominated by herbs (mainly the Asteraceae, Chenopodiaceae, and Poaceae families) rather than trees or shrubs in both the LGM and the Holocene (Sun et al., 1997; Jiang et al., 2013, 2014; Zhao and Ding, 2014; Yang et al., 2015, Fig. 5). Modern plant surveys from both the Chinese Loess Plateau and other regions have shown that (i) a large number of species investigated in the Asteraceae and Poaceae families show a C_{max} of C_{29} or C_{31} (Martin-Smith and Subramanian, 1967; Gnecco et al., 1989; Maffi, 1996; Schwark et al., 2002; Bi et al., 2005; Liu and Huang, 2005), and (ii) several common species studied in the Chenopodiaceae family are characterized by a C_{max} of C_{27} or C_{29} (Liu and Huang, 2005; Carr et al., 2014). All these observations are different from the general assumption that grasses are predominant of C_{31} and C_{33}.

Therefore the long-chain ratios (C_{27}/C_{31}, C_{29}/C_{31}, and $(C_{27}+C_{29})/(C_{31}+C_{33})$) in Chinese loess cannot be used to reflect relative input of woody plants and grasses. Instead, they may mainly reflect changes in the species composition of the steppe vegetation on the Loess Plateau. For a better understanding of leaf wax *n*-alkanes in Chinese loess, further studies are required to investigate the *n*-alkane distributions in both the major plant species and their associated surface soils on the Chinese Loess Plateau.

6. Conclusions

Leaf wax *n*-alkanes in Chinese loess show a bimodal distribution between C_{14} and C_{33} with maxima at C_{14} or C_{16} and at C_{31} or C_{33}, indicating both terrestrial plant and microbial sources. The L/H variations coincide with climate changes both temporally and spatially, i.e. the higher L/H ratio the warmer and wetter climate and vice versa. Thus the L/H ratio in Chinese loess is a reliable proxy for paleoclimate. The temporal and spatial changes in long-chain *n*-alkane ratios (C_{27}/C_{31}, C_{29}/C_{31}, and $(C_{27}+C_{29})/(C_{31}+C_{33})$) are at odds with pollen records (AP/NAP), indicating that the generally used woody plant proxies (C_{27} and C_{29}) and grass proxies (C_{31} and C_{33}) are not applicable to Chinese loess. As steppe prevailed on the Chinese Loess Plateau both in the LGM and the Holocene, the long-chain *n*-alkane ratios may mainly reflect changes in the species composition of local vegetation.

Acknowledgements

This study was supported by the Strategic Priority Research Program of the Chinese Academy of Sciences (Grants XDA05120204 and XDB03020503), and the National Natural Science Foundation of China (Grants 41172157 and 41472318). We thank Shaohua Feng, Zuoling Chen, Shujun Zhao, and Chenxi Xu for the assistance in the field, and Qing Sun, Guoqiang Chu, and Manman Xie for help in the laboratory and for valuable discussions. We are grateful to two anonymous reviewers for their constructive comments and to Norm Catto and Slobodan Marković for editorial handling.

References

Albro, P.W., 1976. Bacterial waxes. In: Kolattukudy, P.E. (Ed.), Chemistry and Biochemistry of Natural Waxes. Elsevier, Amsterdam, pp. 419–439.
Bai, Y., Fang, X.M., Nie, J.S., Wang, Y.L., Wu, F.L., 2006. Distribution of aliphatic ketones in Chinese soils: potential environmental implications. Organic Geochemistry 37, 860–869.
Bai, Y., Fang, X.M., Nie, J.S., Wang, Y.L., Wu, F.L., 2009. A preliminary reconstruction of the paleoecological and paleoclimatic history of the Chinese Loess Plateau from the application of biomarkers. Palaeogeography, Palaeoclimatology, Palaeoecology 271, 161–169.
Bi, X., Sheng, G., Liu, X., Li, C., Fu, J., 2005. Molecular and carbon and hydrogen isotopic composition of *n*-alkanes in plant leaf waxes. Organic Geochemistry 36, 1405–1417.
Buggle, B., Wiesenberg, G.L.B., Glaser, B., 2010. Is there a possibility to correct fossil *n*-alkane data for postsedimentary alteration effects? Applied Geochemistry 25, 947–957.
Bush, R.T., McInerney, F.A., 2013. Leaf wax *n*-alkane distributions in and across modern plants: implications for paleoecology and chemotaxonomy. Geochimica et Cosmochimica Acta 117, 161–179.
Carr, A.S., Boom, A., Grimes, H.L., Chase, B.M., Meadow, M.E., Harris, A., 2014. Leaf wax *n*-alkane distributions in arid zone South African flora: environmental controls, chemotaxonomy and palaeoecological implications. Organic Geochemistry 67, 72–84.
Conte, M.H., Weber, J.C., 2002. Plant biomarkers in aerosols record isotopic discrimination of terrestrial photosynthesis. Nature 417, 639–641.
Cranwell, P.A., 1973. Chain-length distribution of *n*-alkanes from lake sediments in relation to post-glacial environmental change. Freshwater Biology 3, 259–265.
Derbyshire, E., Kemp, R., Meng, X., 1995. Variations in loess and palaeosol properties as indicators of palaeoclimatic gradients across the Loess Plateau of North China. Quaternary Science Reviews 14, 681–697.
Ding, Z.L., Ren, J.Z., Yang, S.L., Liu, T.S., 1999. Climate instability during the penultimate glaciation: evidence from two high-resolution loess records, China. Journal of Geophysical Research 104, 20123–20132.

Ding, Z.L., Derbyshire, E., Yang, S.L., Yu, Z.W., Xiong, S.F., Liu, T.S., 2002. Stacked 2.6-Ma grain size record from the Chinese loess based on five sections and correlation with the deep-sea $\delta^{18}O$ record. Paleoceanography 17, 5-1–5-21.

Eglinton, G., Hamilton, R.J., 1967. Leaf epicuticular waxes. Science 156, 1322–1335.

Eglinton, T.I., Eglinton, G., 2008. Molecular proxies for paleoclimatology. Earth and Planetary Science Letters 275, 1–16.

FAO, 1988. FAO/Unesco Soil Map of the World, Revised Legend, with Corrections and Updates. World Soil Resources Report 60. FAO, Rome.

Freeman, K.H., Colarusso, L.A., 2001. Molecular and isotopic records of C_4 grassland expansion in the late miocene. Geochimica et Cosmochimica Acta 65, 1439–1454.

Gagosian, R.B., Peltzer, E.T., Zafiriou, O.C., 1981. Atmospheric transport of continentally derived lipids to the tropical North Pacific. Nature 291, 312–314.

Gelpi, E., Schneider, H., Mann, J., Oró, T., 1970. Hydrocarbons of geochemical significance in microscopic algae. Phytochemistry 9, 603–612.

Gnecco, S., Bartulin, J., Becerra, J., Marticorena, C., 1989. *n*-Alkanes from Chilean Euphorbiaceae and Compositae species. Phytochemistry 28, 1254–1256.

Gocke, M., Kuzyakov, Y., Wiesenberg, G.L.B., 2010. Rhizoliths in loess – evidence for post-sedimentary incorporation of root-derived organic matter in terrestrial sediments as assessed from molecular proxies. Organic Geochemistry 41, 1198–1206.

Grimalt, J.O., Torras, E., Albaigés, J., 1988. Bacterial reworking of sedimentary lipids during sample storage. Organic Geochemistry 13, 741–746.

Han, J., Calvin, M., 1969. Hydrocarbon distribution of algae and bacteria, and microbiological activity in sediments. Proceedings of the National Academy of Sciences of the United States of America 64, 436–443.

Huang, C.C., Pang, J., Chen, S., Su, H., Han, J., Cao, Y., Zhao, W., Tan, Z., 2006. Charcoal records of fire history in the Holocene loess–soil sequences over the southern Loess Plateau of China. Palaeogeography, Palaeoclimatology, Palaeoecology 239, 28–44.

Huang, Y., Bol, R., Harkness, D.D., Ineson, P., Eglinton, G., 1996. Post-glacial variations in distributions, ^{13}C and ^{14}C contents of aliphatic hydrocarbons and bulk organic matter in three types of British acid upland soils. Organic Geochemistry 24, 273–287.

Johnson, R.W., Calder, J.A., 1973. Early diagenesis of fatty acids and hydrocarbons in a salt marsh environment. Geochimica et Cosmochimica Acta 37, 1943–1955.

Jia, G., Rao, Z., Zhang, J., Li, Z., Chen, F., 2013. Tetraether biomarker records from a loess-paleosol sequence in the western Chinese Loess Plateau. Frontiers in Microbiology 4. http://dx.doi.org/10.3389/fmicb.2013.00199.

Jia, R., Yan, B., Li, R., Fan, G., Lin, B., 1996. Characteristics of magnetotactic bacteria in Duanjiapo loess section, Shaanxi Province and their environment significance. Science China D Earth Science 39, 478–485.

Jiang, H., Ding, Z., 2005. Temporal and spatial changes of vegetation cover on the Chinese Loess Plateau through the last glacial cycle: evidence from spore-pollen records. Review of Palaeobotany and Palynology 133, 23–37.

Jiang, W., Guiot, J., Chu, G., Wu, H., Yuan, B., Hatté, C., Guo, Z., 2010. An improved methodology of the modern analogues technique for palaeoclimate reconstruction in arid and semi-arid regions. Boreas 39, 145–153.

Jiang, W., Cheng, Y., Yang, X., Yang, S., 2013. Chinese Loess Plateau vegetation since the Last Glacial Maximum and its implications for vegetation restoration. Journal of Applied Ecology 50, 440–448.

Jiang, W., Yang, X., Cheng, Y., 2014. Spatial patterns of vegetation and climate on the Chinese Loess Plateau since the Last Glacial Maximum. Quaternary International 334–335, 52–60.

Kolattukudy, P.E., 1976a. Introduction to natural waxes. In: Kolattukudy, P.E. (Ed.), Chemistry and Biochemistry of Natural Waxes. Elsevier, Amsterdam, pp. 1–12.

Kolattukudy, P.E., 1976b. Biochemistry of plant waxes. In: Kolattukudy, P.E. (Ed.), Chemistry and Biochemistry of Natural Waxes. Elsevier, Amsterdam, pp. 290–334.

Kukla, G., 1987. Loess stratigraphy in central China. Quaternary Science Reviews 6, 191–219.

Ladygina, N., Dedyukhina, E.G., Vainshtein, M.B., 2006. A review on microbial synthesis of hydrocarbons. Process Biochemistry 41, 1001–1014.

Liu, J., Chen, T., Nie, G., Song, C., Guo, Z., Li, K., Gao, S., Qiao, Y., Ma, Z., 1994. Dating and reconstruction of the high resolution time series in the Weinan loess section of the last 150,000 years. Quaternary Sciences 6, 193–201 (in Chinese with English abstract).

Liu, T., Ding, Z., 1998. Chinese loess and the paleomonsoon. Annual Review of Earth and Planetary Sciences 26, 111–145.

Liu, W., Huang, Y., 2005. Compound specific D/H ratios and molecular distributions of higher plant leaf waxes as novel paleoenvironmental indicators in the Chinese Loess Plateau. Organic Geochemistry 36, 851–860.

Liu, W., Huang, Y., An, Z., Clements, S.C., Li, L., Prell, W.L., Ning, Y., 2005. Summer monsoon intensity controls C_4/C_3 plant abundance during the last 35 ka in the Chinese Loess Plateau: carbon isotope evidence from bulk organic matter and individual leaf waxes. Palaeogeography, Palaeoclimatology, Palaeoecology 220, 243–254.

Liu, W.G., Huang, Y.S., 2008. Reconstructing *in-situ* vegetation dynamics using carbon isotopic composition of biopolymeric residues in the central Chinese Loess Plateau. Chemical Geology 249, 348–356.

Lu, Y.C., Wang, X.L., Wintle, A.G., 2007. A new OSL chronology for dust accumulation in the last 130,000 yr for the Chinese Loess Plateau. Quaternary Research 67, 152–160.

Luo, P., Peng, P.A., Lü, H.Y., Zheng, Z., Wang, X., 2012. Latitudinal variations of CPI values of long-chain *n*-alkanes in surface soils: evidence for CPI as a proxy of aridity. Science China Earth Sciences 55, 1134–1146.

Maffi, M., 1996. Chemotaxonomic significance of leaf wax alkanes in the Gramineae. Biochemical Systematics and Ecology 24, 53–64.

Maher, B.A., Thompson, R., 1995. Paleorainfall reconstructions from pedogenic magnetic susceptibility variations in the Chinese loess and paleosols. Quaternary Research 44, 383–391.

Martin-Smith, M., Subramanian, G., 1967. Surface wax components of five species of Cortaderia (Gramineae)— a chemotaxonomic comparison. Phytochemistry 6, 559–572.

Meyers, P.A., Ishiwatari, R., 1993. Lacustrine organic geochemistry–an overview of indicators of organic matter sources and diagenesis in lake sediments. Organic Geochemistry 20, 867–900.

Meyers, P.A., 2003. Applications of organic geochemistry to paleolimnological reconstructions: a summary of examples from the Laurentian Great Lakes. Organic Geochemistry 34, 261–289.

Peng, X., Jiang, R., Li, R., Dai, S., Liu, T., 2000. Paleo-environmental study on the growth of magnetotactic bacteria and precipitation of magnetosomes in Chinese loess-paleosol sequences. Chinese Science Bulletin 45, 21–25.

Rao, Z.G., Wu, Y., Zhu, Z.Y., Jia, G.D., Henderson, A., 2011. Is the maximum carbon number of long-chain *n*-alkanes an indicator of grassland or forest? Evidence from surface soils and modern plants. Chinese Science Bulletin 56, 1714–1720.

Rehm, H.J., Reiff, I., 1981. Mechanisms and occurrence of microbial oxidation of long-chain alkanes. Advances in Biochemical Engineering 19, 175–215.

Rutter, N.W., Ding, Z.L., 1993. Paleoclimates and monsoon variations interpreted from micromorphogenic features of the Baoji paleosols, China. Quaternary Science Reviews 12, 853–862.

Schwark, L., Zink, K., Lechterbeck, J., 2002. Reconstruction of postglacial to early Holocene vegetation history in terrestrial Central Europe via cuticular lipid biomarkers and pollen records from lake sediments. Geology 30, 463–466.

Sun, X., Song, C., Wang, F., Sun, M., 1997. Vegetation history of the Loess Plateau of China during the last 100,000 years based on pollen data. Quaternary International 37, 25–36.

Sun, J., 2002. Provenance of loess material and formation of loess deposits on the Chinese Loess Plateau. Earth and Planetary Science Letters 203, 845–859.

Svirčev, Z., Marković, S.B., Stevens, T., Codd, G.A., Smalley, I., Simeunović, J., Obreht, I., Dulić, T., Pantelić, D., Hambach, U., 2013. Importance of biological loess crusts for loess formation in semi-arid environments. Quaternary International 296, 206–215.

Voroney, R.P., 2007. The soil habitat. In: Paul, E.A. (Ed.), Soil Microbiology, Ecology, and Biochemistry, third ed. Academic Press, Burlington, USA, pp. 25–49.

Wakeham, S.G., 1990. Algal and bacterial hydrocarbons in particulate matter and interfacial sediment of the Cariaco Trench. Geochimica et Cosmochimica Acta 54, 1325–1336.

Wang, Y.L., Fang, X.M., Bai, Y., Xi, X.X., Zhang, X.Z., Wang, Y.X., 2007. Distribution of lipids in modern soils from various regions with continuous climate. Science in China Series D–Earth Sciences 50, 600–612. http://dx.doi.org/10.1007/s11430-007-2062-9.

Weete, J.D., 1976. Algal and fungal waxes. In: Kolattukudy, P.E. (Ed.), Chemistry and Biochemistry of Natural Waxes. Elsevier, Amsterdam, pp. 349–418.

Wentzel, A., Ellingsen, T.E., Kotlar, H.-K., Zotchev, S.B., Throne-Holst, M., 2007. Bacterial metabolism of long-chain *n*-alkanes. Applied Microbiology Biotechnology 76, 1209–1221.

Xie, S., Chen, F., Wang, Z., Wang, H., Gu, Y., Huang, Y., 2003. Lipid distributions in loess-paleosol sequences from northwest China. Organic Geochemistry 34, 1071–1079.

Xie, S., Guo, J., Huang, J., Chen, F., Wang, H., Farrimond, P., 2004. Restricted utility of $\delta^{13}C$ of bulk organic matter as a record of paleovegetation in some loess–paleosol sequences in the Chinese Loess Plateau. Quaternary Research 62, 86–93.

Yang, M., Zhang, H., Lei, G., Zhang, W., Fan, H., Chang, F., Niu, J., Chen, Y., 2006. Biomarkers in weakly developed paleosol (L_1SS_1) in the Luochuan loess section and reconstructed paleovegetation-environment during the interstade of the last glaciation. Quaternary Sciences 26, 976–984 (in Chinese with English abstract).

Yang, S.L., Ding, Z.L., 2003. Color reflectance of Chinese loess and its implications for climate gradient changes during the last two glacial-interglacial cycles. Geophysical Research Letters 30, 2058. http://dx.doi.org/10.1029/2003GL018346.

Yang, S., Ding, Z., 2008. Advance-retreat history of the East-Asian summer monsoon rainfall belt over Northern China during the last two glacial interglacial cycles. Earth and Planetary Science Letters 274, 499–510.

Yang, S., Ding, Z., Wang, X., Tang, Z., Gu, Z., 2012. Negative $\delta^{18}O$-$\delta^{13}C$ relationship of pedogenic carbonate from northern China indicates a strong response of C_3/C_4 biomass to the seasonality of Asian monsoon precipitation. Palaeogeography, Palaeoclimatology, Palaeoecology 317–318, 32–40.

Yang, S., Ding, Z., 2014. A 249 kyr stack of eight loess grain size records from northern China documenting millennial-scale climate variability. Geochemistry, Geophysics, Geosystems 15, 798–814.

Yang, S., Ding, Z., Gu, Z., 2014. Acetic acid-leachable elements in pedogenic carbonate nodules and links to the East-Asian summer monsoon. Catena 117, 73–80.

Yang, X., Jiang, W., Yang, S., Kong, Z., Luo, Y., 2015. Vegetation and climate changes in the western Chinese Loess Plateau since the Last Glacial Maximum. Quaternary International 372, 58–65.

Zaady, E., Offer, Z.Y., 2010. Biogenic soil crusts and soil depth: a long-term case study from the Central Negev desert highland. Sedimentology 57, 351–358.

Zech, M., Buggle, B., Leiber, K., Marković, S., Glaser, B., Hambach, U., Huwe, B., Stevens, T., Súmegi, P., Wiesenberg, G., Zöller, L., 2009a. Reconstructing Quaternary vegetation history in the Carpathian Basin, SE Europe, using *n*-alkane biomarkers as molecular fossils: problems and possible solutions, potential and limitations. Eiszeitalter und Gegenwart–Quaternary Science Journal 58, 148–155.

Zech, M., Zech, R., Morrás, H., Glaser, B., Zech, W., 2009b. Late Quaternary environmental changes in Misiones, subtropical NE Argentina, deduced from mulitproxy geochemical analyses in a paleosol-sediment sequence. Quaternary International 196, 121–136.

Zech, M., Andreev, A., Zech, R., Müller, S., Hambach, U., Frechen, M., Zech, W., 2010. Quaternary vegetation changes derived from a loess-like permafrost paleosol sequence in northeast Siberia using alkane biomarker and pollen analyses. Boreas 39, 540–550.

Zech, M., Rass, S., Buggle, B., Manfred, L., Zöller, L., 2012. Reconstruction of the late Quaternary paleoenvironments of the Nussloch loess paleosol sequence, Germany, using *n*-alkane biomarkers. Quaternary Research 78, 226–235.

Zeng, F., Xiang, S., Zhang, K., Lu, Y., 2011. Environmental evolution recorded by lipid biomarkers from the Tawan loess–paleosol sequences on the west Chinese Loess Plateau during the late Pleistocene. Environmental Earth Sciences 64, 1951–1963.

Zhang, H.C., Yang, M.S., Zhang, W.X., Lei, G.L., Chang, F.Q., Pu, Y., Fan, H.F., 2008. Molecular fossil and paleovegetation records of paleosol S4 and adjacent loess layers in the Luochuan loess section, NW China. Science in China Series D–Earth Sciences 51, 321–330.

Zhang, Z., Zhao, M., Lu, H., Faiia, A.M., 2003. Lower temperature as the main cause of C_4 plant declines during the glacial periods on the Chinese Loess Plateau. Earth and Planetary Science Letters 214, 467–481.

Zhang, Z., Zhao, M., Eglinton, G., Lu, H., Huang, C.Y., 2006. Leaf wax lipids as paleovegetational and paleoenvironmental proxies for the Chinese Loess Plateau over the last 170 kyr. Quaternary Science Reviews 25, 575–594.

Zhao, S., Ding, Z., 2014. Changes in plant diversity on the Chinese Loess Plateau since the Last Glacial Maximum. Chinese Science Bulletin 59, 4096–4100. http://dx.doi.org/10.1007/s11434-014-0541-x.

Zhong, Y.X., Chen, F.H., An, C.B., Xie, S.C., Huang, X.Y., 2007. Holocene vegetation cover in Qin'an area of western Chinese Loess Plateau revealed by *n*-alkane. Chinese Science Bulletin 52, 1692–1698.